Journal of Mines, Metals and Fuels, *73(8): 2591-2600; 2025. DOI: 10.18311/jmmf/2025/49534*

Print ISSN : 0022-2755

Journal of Mines, Metals and Fuels

Contents available at: *www.informaticsjournals.co.in/index.php/jmmf*

Numerical Investigation of MHD Free Convection Flow Past an Infinite Vertical Plate with Chemical Reaction

G. Deepa[1], A. Sridhar[2], B. S. Surya Prabhavati[3]*, J. Venkata Madhu[4], B. Nagaraju[5], G. Murali[3], S. M. Bhati[6] and S. J. Kokate[6]

[1]*Chaitanya Bharathi Institute of Technology, Gandipet, Hyderabad - 500075, Telangana, India*
[2]*Malla Reddy University, Hyderabad - 500100, Telangana, India*
[3]*Geethanjali College of Engineering and Technology, Hyderabad - 501301, Telangana, India; b.s.s.prabhavati@gmail.com*
[4]*Sreenidhi Institute of Science and Technology, Yamnampet - 501301, Telangana, India*
[5]*Palamuru University, Mahbubnagar - 509001, Telangana, India*
[6]*KBT College of Engineering, Nashik - 422013, Maharashtra, India*

Abstract

The impact of chemical reactions on magnetohydrodynamic free convective fluid flow adjacent to an infinitely long, vertically accelerated plate is a subject of significant interest. This study delves into the intricate interactions between fluid dynamics and magnetic fields, highlighting the complexities introduced by chemical processes. By examining the behaviour of the fluid under these conditions, we aim to provide a comprehensive understanding of the underlying mechanisms at play, which is crucial for advancing theoretical models and practical applications in the field. The study looks into the mass and heat transfer of a viscous fluid across a vertical plate that is encased in a porous material that is fluid-saturated. It generates closed-form solutions to the momentum, energy, and concentration equations using the finite element method. The text provides tabular representations of numerical values of shear stress, heat transfer, and mass transfer at the plate, along with visual depictions of fluid velocity, temperature, and species concentration. In a few specific instances, the outcomes align favorably with the earlier discoveries.

Major Findings: *The study examines MHD free convection near a vertical plate, analysing heat/mass transfer in porous media. Finite element solutions yield velocity, temperature, and concentration profiles. Results match prior work, emphasising chemical reactions' influence on flow and magnetic interactions.*

Keywords: *Chemical Reaction, Finite Element Method, MHD, Natural Convection, Porous Medium*

1.0 Introduction

Free convection, the enhanced flow of a viscous incompressible fluid across an infinite vertical porous plate, has considerable practical relevance in astronomy, geophysics, and engineering. Heat transmission inside buildings and rooms, shown by radiator heating, is a standard instance of heat transfer by free convection. Thermal radiation substantially affects surface heat transfer during convective heat transfer. This is especially

*Author for correspondence

true in free convection issues involving absorbing and releasing fluids. Chemical reactions may significantly modify diffusion rates during convective heat and mass transfer. These reactions may be categorised as homogeneous or heterogeneous, with their rate being proportional to the nth power of the concentration. First-order reactions have a rate that is directly proportional to the concentration. In the natural environment, pure air and water are nonexistent, and contaminants may occur naturally or in conjunction with air or water. Examining these chemical reaction pathways may enhance chemical technologies, including polymer synthesis and food processing.

Recent research on heat and mass transfer in porous media has significantly advanced our understanding of convective flows. Ingham and Pop[1] and Vafai[2] have provided comprehensive reviews of this field, examining factors like variable fluid properties and boundary conditions. Several studies have focused on specific aspects: Kassoy and Zebib[3] analysed viscosity effects on convective instability, while Cheng and Minkowycz[4] explored free convection applications in geothermal systems. Bejan and Khair[5] and Lai and Kulacki[6] investigated buoyancy-driven transfer and viscosity impacts in vertical configurations. Researchers have examined various flow scenarios - Murali[7] studied steady flows with temperature-dependent properties, Yih[8] analysed mixed convection around wedges, and Kumari[9] examined horizontal surfaces. Postelnicu *et al.*[10] and Seddeek[11], and Seddeek and Salem[12] investigated forced convection and chemical reaction effects. Additional contributions include Mohamed[13] work on mixed convection, Alam *et al.*'s[14] combined convection analysis, and Pantokratoras's[15] constant temperature studies. More complex scenarios were addressed by Reddy *et al.*[16], who modelled MHD flows with magnetic effects, building on Sparrow and Cess's[17] foundational MHD research. These collective works have substantially enhanced our knowledge of transport phenomena in porous media, with applications ranging from energy systems to chemical engineering. Previous studies[18-23] have demonstrated diverse practical applications in this field. Meanwhile, researchers in[24-30] successfully employed the finite element method to analyse Magnetohydrodynamic (MHD) heat and mass transfer problems, achieving highly accurate computational results. Further advancements were made in works[31-33], which deepened the fundamental understanding of these coupled transport phenomena through detailed theoretical and numerical investigations.

A lot of problems, especially those that have to do with cooling nuclear and electrical components, specify the wall heat flux. Meltdowns and overheating are major concerns in these kinds of situations. An essential wall model with continuous heat flux is taken into consideration from a practical standpoint. This work, which was motivated by the aforementioned reference work, suggests examining the effects of heat and mass transfer on unsteady MHD free convective fluid flow *via* the finite element method.

2.0 Mathematical Formulation

The primary equations that regulate the incompressible free convective MHD flow and energy transfer when a fluid passes an indefinitely long vertical plate nested in a porous medium under Boussinesq's approximation are provided. The physical coordinate system of this work is as shown in Figure 1.

On the plate, the x-axis is oriented vertically, while the y-axis is oriented perpendicularly.

- At $t' > 0$, the y-axis direction is supplied with a magnetic field that is consistently strong
- Neglect is given to the generated magnetic field
- for time $t' \leq 0$ temperature and concentration are T'_{∞} C'_{∞}

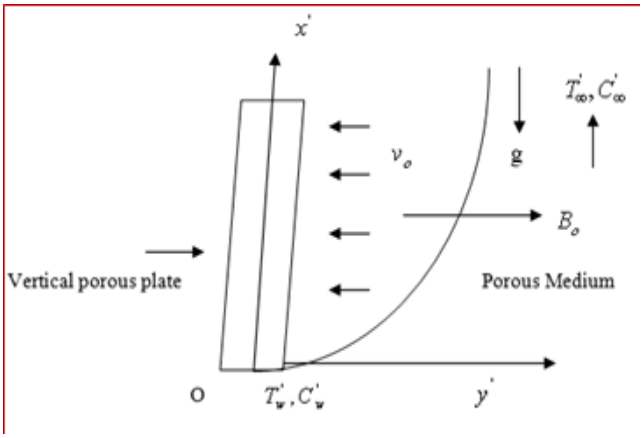


Figure 1. Physical sketch and geometry of the problem.

The following are the flow governing equations.

Continuity Equation

$$\frac{\partial v'}{\partial y'} = 0 \Rightarrow v' = -v'_o \text{ (Constant)} \quad (1)$$

Momentum Equation

$$\frac{\partial u'}{\partial t'} = \nu \frac{\partial^2 u'}{\partial y'^2} - \frac{\sigma B_o^2 u'}{\rho} + g\beta(T' - T'_\infty) + g\beta^*(C' - C'_\infty) - \frac{\nu u'}{K'} \quad (2)$$

Energy Equation

$$\frac{\partial T'}{\partial t'} = \frac{\kappa}{\rho c_p}\frac{\partial^2 T'}{\partial y'^2} + \frac{D_m k_T}{c_S c_p}\frac{\partial^2 C'}{\partial y'^2} \quad (3)$$

Diffusion Equation

$$\frac{\partial C'}{\partial t'} = D\frac{\partial^2 C'}{\partial y'^2} - K'_r C' + \frac{D_m k_T}{T_m}\frac{\partial^2 T'}{\partial y'^2} \quad (4)$$

With the following initial and boundary conditions:

$$t' \le 0 : u' = 0,\ T' = T'_\infty,\ C' = C'_\infty \ \text{for all } y'$$

$$t' > 0 : \left\{ \begin{array}{l} u' = U_o,\ \dfrac{\partial T'}{\partial y'} = -\dfrac{q'}{\kappa'},\ C' = C'_w \ \text{at } y' = 0, \\ u' = 0,\ T' = T'_\infty,\ C' = C'_\infty \ \text{at } y' \to \infty \end{array} \right\} \quad (5)$$

Introducing the following dimensionless quantities:

$$t = \frac{t' U_o^2}{\nu},\ y = \frac{U_o y'}{\nu},\ u = \frac{u'}{U_o},\ \Pr = \frac{\mu C_p}{\kappa},\ Sc = \frac{\nu}{D},$$

$$M = \frac{\sigma B_o^2 \nu}{\rho U_o^2},\ Gr = \frac{\nu g\beta(T'_w - T'_\infty)}{U_o^3},\ Gc = \frac{g\beta^*\nu(C'_w - C'_\infty)}{U_o^3},$$

$$K = \frac{U_o^2 K'}{\nu^2},\ \theta = \frac{T' - T'_\infty}{T'_w - T'_\infty},\ C = \frac{C' - C'_\infty}{C'_w - C'_\infty},\ Du = \frac{D_m k_T (C'_w - C'_\infty)}{c_S c_P (T'_w - T'_\infty)},$$

$$Sr = \frac{D_m k_T (T'_w - T'_\infty)}{\nu T_m (C'_w - C'_\infty)},\ k_r = \frac{K'_r \nu}{U_0^2} \quad (6)$$

Using (6), Equations (2), (3) and (4) are of the following form.

$$\frac{\partial^2 u}{\partial y^2} + (Gr)\theta + (Gc)C = \frac{\partial u}{\partial t} + \left(M + \frac{1}{K}\right)u \quad (7)$$

$$\frac{\partial^2 \theta}{\partial y^2} = (\Pr)\frac{\partial \theta}{\partial t} - (\Pr)(Du)\left(\frac{\partial^2 C}{\partial y^2}\right) \quad (8)$$

$$\frac{\partial^2 C}{\partial y^2} = (Sc)\frac{\partial C}{\partial t} - (Sc)(Sr)\left(\frac{\partial^2 \theta}{\partial y^2}\right) + (Sc)(k_r)C \quad (9)$$

With the following initial and boundary condition

$$t \le 0 : u = 0,\ \theta = 0,\ C = 0 \ \text{for all } y$$

$$t > 0 : \left\{ \begin{array}{l} u = 1,\ \dfrac{d\theta}{dy} = -1,\ C = 1 \ \text{at } y = 0 \\ u = 0,\ \theta = 0,\ C = 0 \ \text{at } y \to \infty \end{array} \right\} \quad (10)$$

Skin friction, Nusselt number and Sherwood number in dimensionless form are as follows.

$$\tau = \frac{\tau'_w}{\rho U_o \nu} = \left(\frac{\partial u}{\partial y}\right)_{y=0} \quad (11)$$

$$Nu = -x\frac{\left(\frac{\partial T'}{\partial y'}\right)_{y'=0}}{T'_w - T'_\infty} \Rightarrow Nu\,\mathrm{Re}_x^{-1} = -\left(\frac{\partial \theta}{\partial y}\right)_{y=0} \quad (12)$$

$$Sh = -x\frac{\left(\frac{\partial C'}{\partial y'}\right)_{y'=0}}{C'_w - C'_\infty} \Rightarrow Sh\,\mathrm{Re}_x^{-1} = -\left(\frac{\partial C}{\partial y}\right)_{y=0} \quad (13)$$

3.0 Method of Solution

Numerical modelling and simulation have simplified, reduced costs, and improved the efficiency of solving mathematical equations. Computer numerical modelling allows for accurate analysis and comparison of solutions with real systems, enabling faster and more effective problem-solving. The Galerkin finite element method, particularly useful in physics and mechanical engineering, can be applied in future research for solving differential equations.

These equations can be found by using the trapezoidal rule.

$$A_1 u_{i-1}^{n+1} + A_2 u_i^{n+1} + A_3 u_{i+1}^{n+1} = A_4 u_{i-1}^n + A_5 u_i^n + A_6 u_{i+1}^n + P^* \quad (18)$$

Now, from equations (8) and (9), the following equations are obtained:

$$B_1\theta_{i-1}^{n+1} + B_2\theta_i^{n+1} + B_3\theta_{i+1}^{n+1} = B_4\theta_{i-1}^{n} + B_5\theta_i^{n} + B_6\theta_{i+1}^{n} + Q^* \quad (19)$$

$$D_1C_{i-1}^{n+1} + D_2C_i^{n+1} + D_3C_{i+1}^{n+1} = D_4C_{i-1}^{n} + D_5C_i^{n} + D_6C_{i+1}^{n} + R^* \quad (20)$$

where

$$A_1 = 2+Ak-6r,\ A_2 = 8+12r,\ A_3 = 2+Ak-6r,\ A_4 = 2-Ak+6r,\ A_5 = 8-12r,$$

$$A_6 = 2-Ak+6r,\ B_1 = 2(\mathrm{Pr})-6r,\ B_2 = 8(\mathrm{Pr})+12r,\ B_3 = 2(\mathrm{Pr})-6r,\ B_4 = 2(\mathrm{Pr})+6r,$$

$$B_5 = 8(\mathrm{Pr})-12r,\ B_6 = 2(\mathrm{Pr})+6r,\ D_1 = 2(Sc)-6r-(k_r)(Sc)k,\ D_2 = 8(Sc)+12r+4(k_r)(Sc)rh,$$

$$D_3 = 2(Sc)-6r-(k_r)(Sc)k,\ D_4 = 2(Sc)+6r+(k_r)(Sc)k,\ D_5 = 8(Sc)-12r-4(k_r)(Sc)rh,$$

$$D_6 = 2(Sc)+6r+(k_r)(Sc)k,\ P^* = 12kP = 12k(Gr)\theta_i^j + 12k(Gc)C_i^j,$$

$$Q^* = 12kQ = 12k(\mathrm{Pr})(Du)\left(\frac{\partial^2 C_i^j}{\partial y^2}\right),\ R^* = 12kR = 12k(Sc)(Sr)\left(\frac{\partial^2 \theta_i^j}{\partial y^2}\right)$$

Here, $r = \frac{k}{h^2}$, Index i-space and j-time. By taking $i = 1(1)n$ in (18), (19) and (20) and from conditions (10), then the system will be of the following form

$$A_iX_i = B_i \quad for\ i = 1(1)n \quad (21)$$

The Thomas algorithm is employed to solve the system of equations governing concentration, temperature, and velocity. Numerical solutions for these problems are obtained using a C program, which was executed with refined step sizes h and k to validate the convergence and stability of the GFEM. The results showed negligible variations in the values of u, ϕ, and C, confirming the method's robustness and reliability.

4.0 Results and Discussions

The study looks at the effects of several parameters. An innovative way to solve heat and mass transfer issues is the Magnetohydrodynamics-Driven Heat and Mass Transfer Problem-Solving System. Advanced thermal management algorithms, fluid dynamics control, and the principles of magnetohydrodynamics are used to control the behaviour of electrically conducting fluids in a regulated setting. The technology allows for improved control over heat and mass transport processes by using a magnetic field generator to precisely modify magnetic fields. Efficiency is increased by the fluid dynamics control system, which maximises circulation, turbulence, and velocity. The thermal management algorithms of the system precisely and effectively meet thermal requirements by continuously monitoring and analysing temperature differentials. Because of its adaptability and reactivity to feedback loops, the system is a useful addition to power generation systems, where higher energy output is directly correlated with increased efficiency.

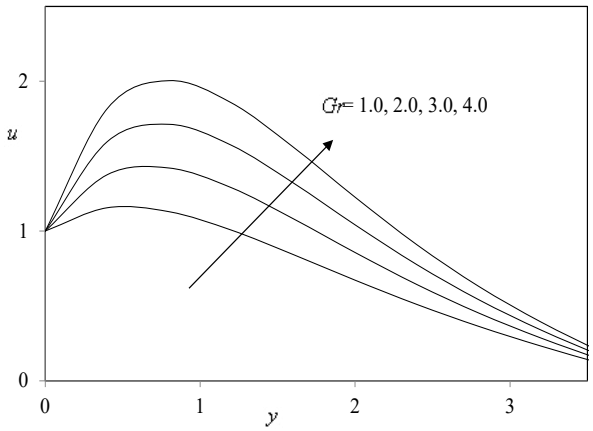


Figure 2. Effect of Grashof number G_r on velocity profiles u.

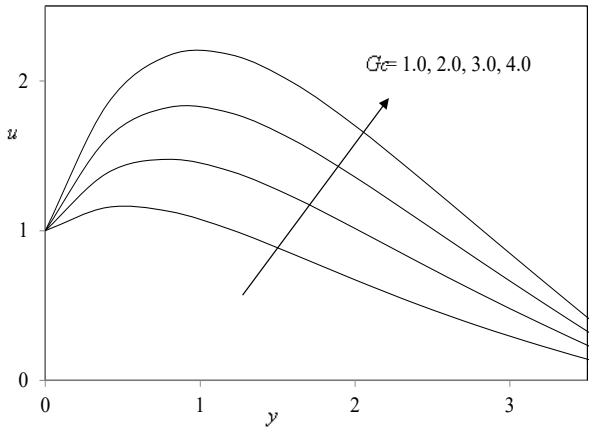


Figure 3. Effect of modified Grashof number G_c on velocity profiles u.

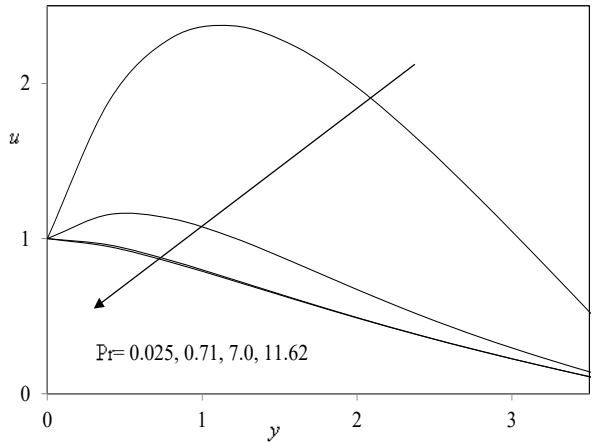


Figure 4. Effect of Prandtl number P_r on velocity profiles u.

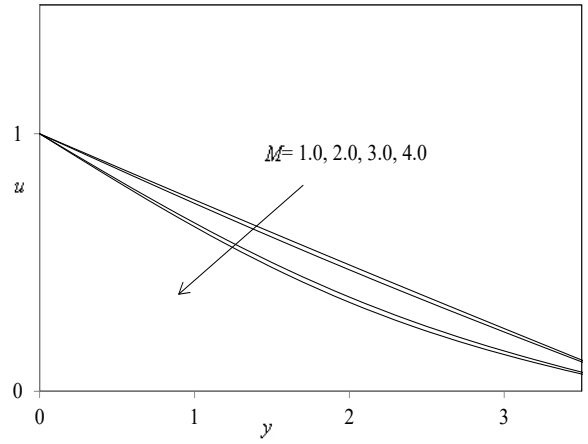


Figure 6. Effect of Hartmann number M on velocity profiles u.

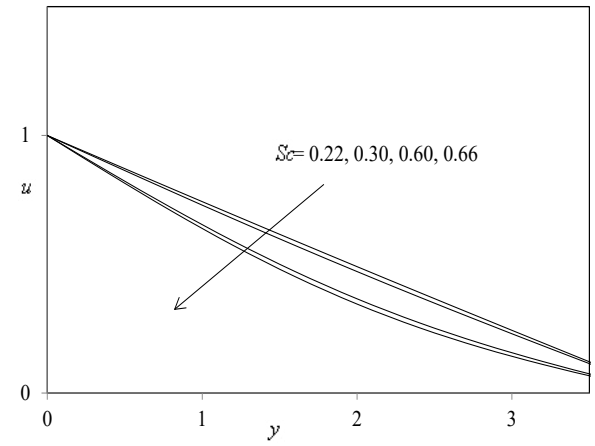


Figure 5. Effect of Schmidt number S_c on velocity profiles u.

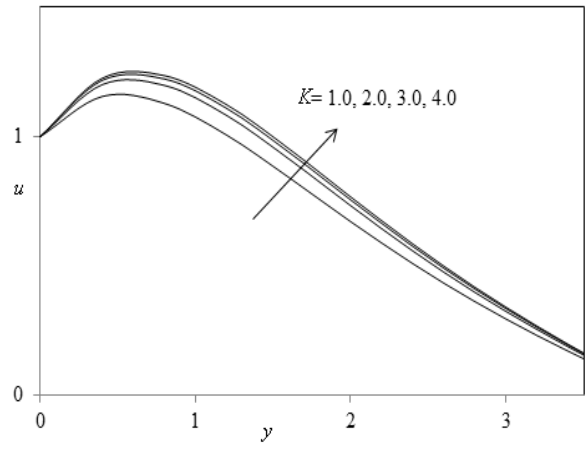


Figure 7. Effect of permeability parameter K on velocity profiles u.

The velocity of the flow field changes with the variation of nine parameters. The primary elements impacting the velocity include free convection current, Grashof number, mass transfer, parameter accelerating effect, and Prandtl number. The free convection current increases velocity at all points, while the Grashof number effects mass transfer, which was shown in Figures 2 and 3. The Prandtl number decreases velocity at all sites in the flow field which as shown in Figure 4. As shown in Figures 5 and 6, the flow field's velocity is influenced by various factors, including the Schmidt number, Hartmann number, porous medium parameter, Soret and Dufour numbers, and chemical reaction parameter. The Schmidt number decreases at every point, while the Hartmann number increases due to the Lorentz force, a resistive force that impedes fluid flow. Figure 7 demonstrates that the thickness of the boundary layer decreases with increasing Hartmann number, while flow properties can be controlled by a magnetic field.

From Figure 8, the Soret and Dufour numbers also impact the velocity field, with a significant decrease in velocity profiles expected as the number increases. The chemical reaction parameter significantly impacts velocity profiles, with a peak suggesting that the fluid's body near the surface experiences maximum velocity, but not at the surface. As shown in Figure 9, the case study

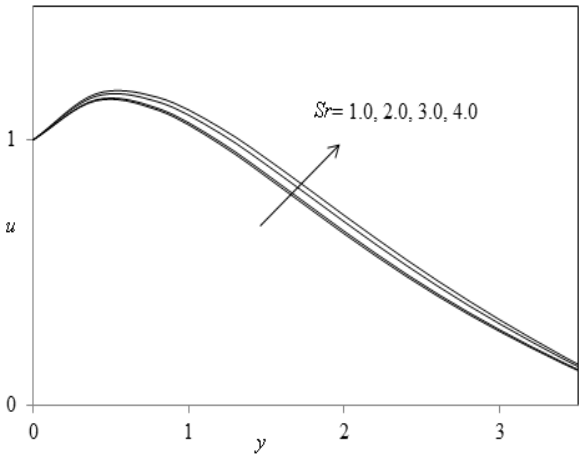


Figure 8. Effect of Soret number S_r on velocity profiles u.

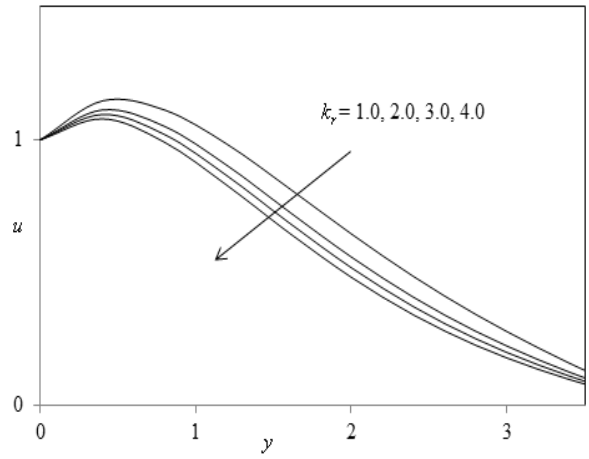


Figure 10. Effect of Chemical Reaction Parameter k_r on velocity profiles u.

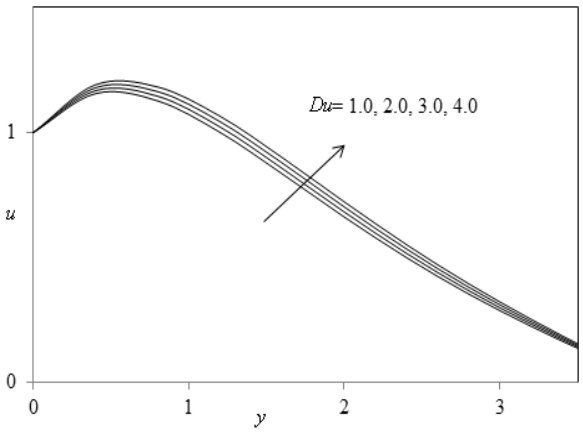


Figure 9. Effect of Dufour number Du on velocity profiles u.

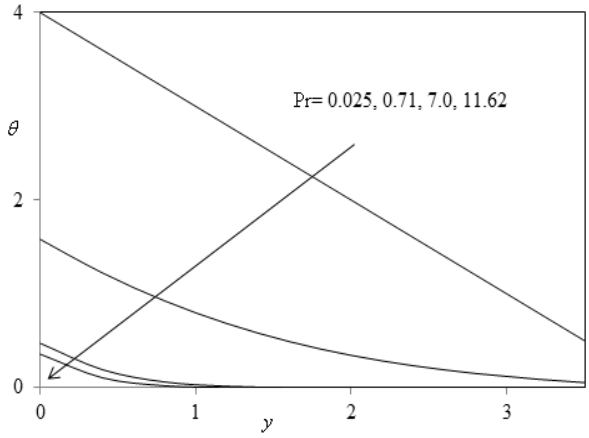


Figure 11. Effect of Prandtl number P_r on temperature profiles θ.

highlights the importance of considering the presence of harmful chemical reactions in the flow field.

The study reveals that the velocity of a fluid increases with the increase in Dufour and Soret numbers, and the chemical reaction parameter significantly impacts these profiles. As shown in Figure 10, the case study focuses on a harmful chemical reaction, which results in a significant decrease in velocity profiles. The presence of a peak indicates that the fluid's body near the surface experiences maximum velocity, but not at the surface. The temperature of the flow field also changes significantly with flow characteristics like Prandtl number and Dufour number. Mercury's temperature field curve is linear, indicating its sensitivity to temperature changes. Mercury is found to be the best laboratory solution for sustaining temperature differences. As shown in Figure 11, air can be a more suitable and affordable replacement for machinery if proper temperature control is practised.

As shown in Figure 12, the concentration of the flow field is significantly influenced by flow parameters like Sc, Sr, and Kr. The Soret number does not directly affect velocity and temperature profiles. As shown in Figure 13, the Soret number tends to decay, overshooting uniform concentration near the boundary. As shown in Figure 14, Chemical reaction parameters also impact concentration profiles, with concentration decreasing with increased

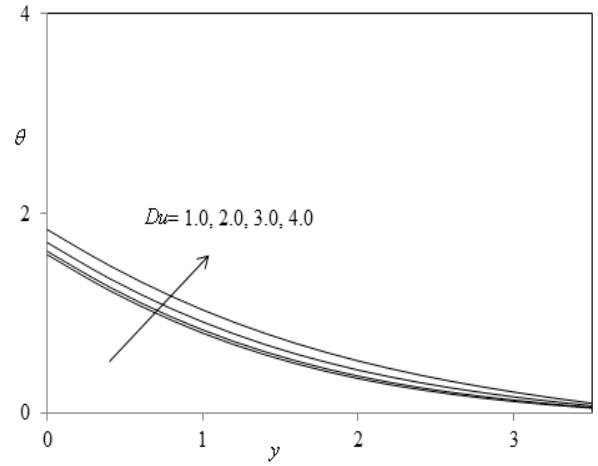


Figure 12. Effect of Dufour number *Du* on temperature profiles θ.

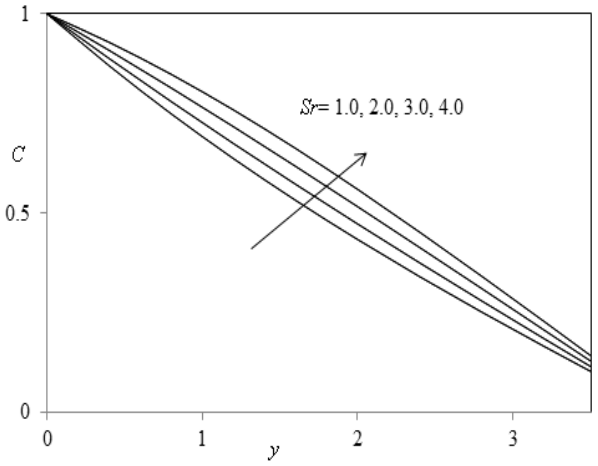


Figure 14. Effect of Soret number S_r on concentration profiles *C*.

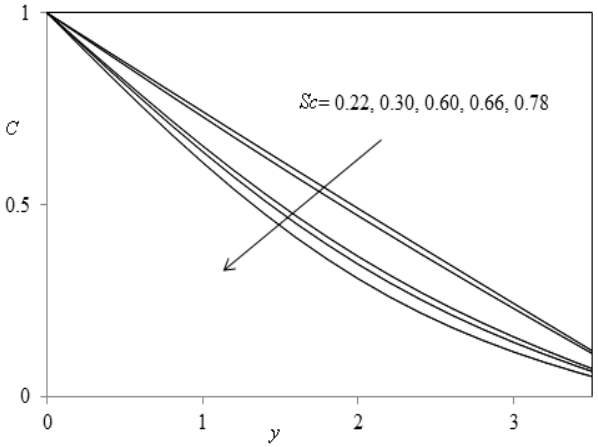


Figure 13. EEffect of Schmidt number S_c on concentration profiles *C*.

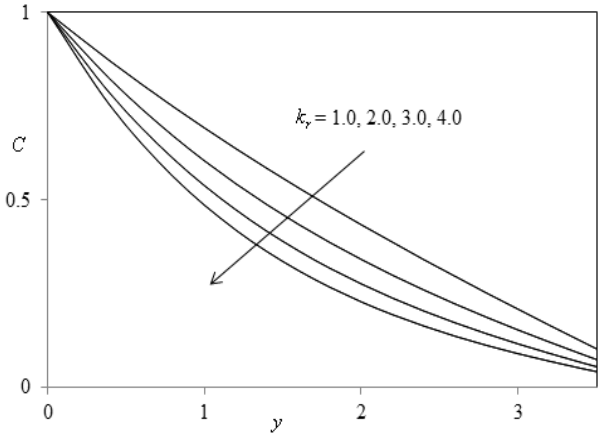


Figure 15. Effect of chemical reaction parameter k_r on concentration profiles *C*.

Table 1. Variation of numerical values of skin friction (τ)

G_r	G_c	P_r	S_c	M	K	S_r	Du	k_r	τ
1.0	1.0	0.71	0.22	2.0	1.0	1.0	1.0	1.0	1.5879
2.0	1.0	0.71	0.22	2.0	1.0	1.0	1.0	1.0	1.8742
1.0	2.0	0.71	0.22	2.0	1.0	1.0	1.0	1.0	1.9873
1.0	1.0	7.00	0.22	2.0	1.0	1.0	1.0	1.0	1.2590
1.0	1.0	0.71	0.60	2.0	1.0	1.0	1.0	1.0	1.3586
1.0	1.0	0.71	0.22	4.0	1.0	1.0	1.0	1.0	1.1167
1.0	1.0	0.71	0.22	2.0	2.0	1.0	1.0	1.0	1.6540
1.0	1.0	0.71	0.22	2.0	1.0	2.0	1.0	1.0	1.7412
1.0	1.0	0.71	0.22	2.0	1.0	1.0	2.0	1.0	1.6984
1.0	1.0	0.71	0.22	2.0	1.0	1.0	1.0	2.0	1.3695

reaction. As shown in Figure 15, the Schmidt number shrinks with increasing Schmidt number.

As shown in Table 1, the study reveals that skin friction increases with increasing values of a variable, with the behaviour reversed with increasing values of a variable. As shown in Table 2, the Nusselt number also increases with increasing values, while the Sherwood number also increases with increasing values. Table 3 presents a comparative analysis between the obtained skin-friction values and those reported in earlier works, revealing close numerical correspondence that verifies the reliability of the current findings.

Table 2. Variation of Nusselt number (*Nu)* for different values of P_r, *Du* and λ

P_r	*Du*	*Nu*
0.71	1.0	1.2875
7.00	1.0	1.0067
0.71	2.0	1.3481

Table 3. Variation of Sherwood number (*Sh*) for different values of *Sc, Sr,* k_r and λ

Sc	*Sr*	k_r	*Sh*
0.22	1.0	1.0	1.0598
0.30	1.0	1.0	0.8436
0.22	2.0	1.0	1.2597
0.22	1.0	2.0	0.7694

Table 4. Comparison of present Skin – Friction results (τ_1) with the previous Skin – Friction results (τ^*_1)

G_r	P_r	*M*	τ_1	τ^*_1
1.0	0.71	2.0	1.2254	1.2197
2.0	0.71	2.0	1.3592	1.3465
1.0	0.71	2.0	0.9987	0.9954

5.0 Conclusions

A thorough numerical parametric analysis is carried out for the numerical solutions of nonlinear equations, and the findings are shown as graphs. This is done to highlight unique aspects of the solutions. Thus, numerical solutions were achieved through the use of the finite element approach. Other than that, the results show that it is a suitable approach for solving the current challenges. The findings also demonstrate that in a destructive reaction, the concentration of particles is increased by higher-order chemical reactions, whereas in a generative process, it is decreased. A tight correspondence between the present skin friction results and the previous results.

6.0 References

1. Ingham DB, Pop I. Transport phenomena in porous media III, Elsevier, Oxford; 2005.
2. Vafai K. Handbook of Porous media (2nd edition), Taylor and Francis, New York; 2005. https://doi.org/10.1201/9780415876384
3. Kassoy DR, A. Zebib. Variable viscosity effects on the onset of convection in porous media. Phy Fluids. 1975; 18(12):1649-1651. https://doi.org/10.1063/1.861083
4. Cheng P, Minkowycz WJ. Free convection about a vertical flat plate embedded in a porous medium with application to heat transfer from a dike. J Geophys Res. 1977; 82(14):2040-20444. https://doi.org/10.1029/JB082i014p02040
5. Bejan A, Khair KR. Heat and mass transfer by natural convection in a porous medium. Int J Heat Mass Transf. 1985; 28(5):909-918. https://doi.org/10.1016/0017-9310(85)90272-8
6. Lai FC, Kulacki FA. The effect of variable viscosity on convective heat transfer along a vertical surface in a saturated porous medium. Int J Heat Mass Transf. 1990; 33(5):1028-1031. https://doi.org/10.1016/0017-9310(90)90084-8
7. Murali G, Venkata Madhu J, Deepa G. *et al.* Hall current and MHD impacts on a 3D Maxwell nanofluid flow across a porous stretching surface. Theor Math Phys. 2025; 223:899–914. https://doi.org/10.1134/S0040577925060030
8. Yih KA. Coupled heat and mass transfer in mixed convection over a wedge with variable wall temperature and concentration in porous media: The entire regime. Int Comm Heat Mass Transf. 1998; 25(8):1145-1158. https://doi.org/10.1016/S0735-1933(98)00105-5
9. Kumari M. Variable viscosity effects on free and mixed convection boundary-layer flow from a horizontal surface in a saturated porous medium - Variable heat flux. Mech Res Comm. 2001; 28(3):339-348. https://doi.org/10.1016/S0093-6413(01)00182-3

10. Postelnicu A, Groşan T, Pop I. The effect of variable viscosity on forced convection flow past a horizontal flat plate in a porous medium with internal heat generation. Mech Res Comm. 2001; 28(3):331-337. https://doi.org/10.1016/S0093-6413(01)00181-1
11. Seddeek MA. Finite-element method for the effects of chemical reaction, variable viscosity, thermophoresis and heat generation/absorption on a boundary-layer hydromagnetic flow with heat and mass transfer over a heat surface. Acta Mech. 2005; 177(1-4):1-18. https://doi.org/10.1007/s00707-005-0249-8
12. Seddeek MA, Salem AM. Laminar mixed convection adjacent to vertical continuously stretching sheets with variable viscosity and variable thermal diffusivity. Heat Mass Transf. 2005; 41(12):1048-1055. https://doi.org/10.1007/s00231-005-0629-6
13. Ali ME. The effect of variable viscosity on mixed convection heat transfer along a vertical moving surface. Int J Therm Sci. 2005; 45(1):60-69. https://doi.org/10.1016/j.ijthermalsci.2005.04.006
14. Alam MS, Rahman MM, Samad MA. Numerical study of the combined free-forced convection and mass transfer flow past a vertical porous plate in a porous medium with heat generation and thermal diffusion. Nonlinear Anal: Model Control. 2006; 11(4):331-343. https://doi.org/10.15388/NA.2006.11.4.14737
15. Pantokratoras A. The Falkner–Skan flow with constant wall temperature and variable viscosity. Int J Therm Sci. 2006; 45(4):378-389. https://doi.org/10.1016/j.ijthermalsci.2005.06.004
16. Reddy GVR, Murthy CVR, Reddy NB. Mixed convective MHD flow and mass transfer past an accelerated infinite vertical porous plate. Math Appl Sci Tech. 2009; 1(1):65-74.
17. Sparrow EM, Cess RD. The effect of a magnetic field on free convection heat transfer. Int J Heat Mass Transf. 1961; 3(4):267-274. https://doi.org/10.1016/0017-9310(61)90042-4
18. Alam S, Rahman MM. Dufour and Soret effects on MHD free convective heat and mass transfer flow past a vertical porous flat plate embedded in a porous medium. J Noval Arch Marine Eng. 1970; 2(1):55-65. https://doi.org/10.3329/jname.v2i1.2030
19. Gadipally D, Gundagani M. Analysis of Soret and Dufour effects on unsteady MHD convective flow past a semi-infinite vertical porous plate via finite difference method. Int J Appl Phy Math. 2014; 4(5):332-344. https://doi.org/10.7763/IJAPM.2014.V4.306
20. Kirubaharan DR, Subhashini AD, Murali G. Study of three dimensional Casson-nanofluid flow due to a linear porous stretching sheet in the presence of double diffusion effects. Adv Sys Sci Appl. 2024; 24(3): 90-103. https://doi.org/10.25728/assa.2024.2024.03.1539
21. Gundagani M, Babu N, Gadially D, Bhati SM, Sanjay C, Kasturi VN. Study of nano-Powell-Erying fluid flow past a porous stretching sheet by the effects of MHD, thermal and mass convective boundary conditions. J Umm Al-qura Univ Eng Archit. 2024; 15(3):271-281. https://doi.org/10.1007/s43995-024-00056-2
22. Murali G, Deepa G, Madhu JV, Kasturi VN, Bhati SM, Babu NN. Three dimensional chemically reacting Oldroyd-B fluid + nanofluid flow in presence of thermophoresis and Brownian Motion effects. Discont Nonlin Complex. 2025; 14(2):373-388. https://doi.org/10.5890/DNC.2025.06.010
23. Murali, G., Deepa, G., Nirmala Kasturi, V., Poornakantha, T., Joint effects of thermal diffusion and diffusion thermo on MHD three dimensional nanofluid flow towards a stretching sheet. Math Model Engineering. 2023; 9(4):130-143. 2023. https://doi.org/10.21595/mme.2023.23590
24. Murali, G, Lakshmi, P, Amarnath, M. *et al*. Three-dimensional MHD flow of a radiative Eyring–Powell nanofluid: Exploring Hall effects and heat transfer. Theor Math Phys. 2025; 223: 1070–1086. https://doi.org/10.1134/S0040577925060170
25. Bhati SM, Murali G, Sanjay C. Law of electric fields via bianchi identities. J Appl Sci Eng. 2022; 25(4): 759-762. https://doi.org/10.6180/jase.202208_25(4).0011
26. Tanuku PK, Mamidi LP, Gundagani M. Modelling and analysis of three-dimensional chemically reacting, radiating Casson-nanofluid flow: Thermophoresis and Brownian motion effects. Acta Polytech. 2024; 64(5):455-463. https://doi.org/10.14311/AP.2024.64.0455
27. Murali G, Madhu JV, Deepa G, Suresh P, Nagaraju B. Three-dimensional oldroyd-B fluid flow past a stretching surface with magnetic field, Nanofluid particles and Cattaneo-Christov double diffusion effects. Johnson Matthey Technology Review. 2025; 69(2):299 – 320. https://doi.org/10.1595/205651325X17375408788409.
28. Mebarek-Oudina F, Dharmaiah G, Prasad JLR, Vaidya H, Kumari MA. Investigation of magnetohydrodynamic Burgers' fluid flow under cylinder stretching: Effects of internal heat generation and absorption. Int J Thermophys. 2025; 25:100986. https://doi.org/10.1016/j.ijft.2024.100986

29. Gundagani M, Javvaji V, Gadipalli D, Pallerla S, Al-Mdallal Q, Bhati S. A numerical study on MHD 3-D Casson-nanofluid flow past an exponentially stretching sheet with double Cattaneo-Christov Diffusion Effects. Rev Int Métodos Numér Cálc Diseñoing. 2025; 41(2):21. https://www.scipedia.com/public/Gundagani_et_al_2025a
30. Fayz-Al-Asad Md, Mebarek-Oudina F, Vaidya H, Hasan MS, Sarker MMA, Ismail AI. Finite element analysis for magneto-convection heat transfer performance in vertical wavy surface enclosure: Fin size impact. Front Heat Mass Transf. 2024; 22(3):817-837. https://doi.org/10.32604/fhmt.2024.050814
31. Sivaiah S, Gundagani M, Karanamu MP. Analysis of heat and mass transfer effects on an isothermal vertical oscillating plate. Walailak J Sci Tech. (WJST). 2012; 9(4):407–415. https://wjst.wu.ac.th/index.php/wjst/article/view/451
32. Liu I-Chung, Andersson HI. Heat transfer over a bidirectional stretching sheet with variable thermal conditions. Int J Heat Mass Transf. 2008; 51(15-16):4018-4024. https://doi.org/10.1016/j.ijheatmasstransfer.2007.10.041
33. Nagasmitha BR, Nagendramma V, Ahmed N, Marutamanikandan S, Murali G. Analytical study of nonlinear behavior and convection patterns in Darcy-Brinkman porous medium with Maxwell-Cattaneo ferroconvection. J Mines Met Fuels. 2025; 437-445. https://doi.org/10.18311/jmmf/2025/47828